Solid State Ionics 183 (2011) 48–53

Contents lists available at ScienceDirect

Solid State Ionics

journal homepage: www.elsevier.com/locate/ssi

Synthesis of garnet-type $Li_{7-x}La_3Zr_2O_{12-1/2x}$ and its stability in aqueous solutions

Yuta Shimonishi, Akiharu Toda, Tao Zhang, Atsushi Hirano, Nobuyuki Imanishi, Osamu Yamamoto, Yasuo Takeda *

Department of Chemistry for Materials, Graduate School of Engineering, Mie University, 1577 Kurimamachiya-cho, Tsu, 514-8507, Japan

ARTICLE INFO

Article history:
Received 24 September 2010
Received in revised form 21 December 2010
Accepted 23 December 2010
Available online 21 January 2011

Keywords:
Lithium air cell
Lithium ion conducting sold
Garnet-type structure
Water stable lithium metal electrode

ABSTRACT

The garnet-type cubic and tetragonal phases with respective high and low lithium ion conductivity were synthesized using precursors prepared by a sol–gel method. The electrical conductivities of the bulk and grain boundary of the cubic phase were estimated from impedance spectra to be 5.69×10^{-4} and 1.39×10^{-4} S cm^{-1} at 25 °C, respectively. The garnet-type cubic phase was stable in a saturated solution of LiCl, and no changes in the XRD pattern or electrical conductivity were observed for a sample immersed in saturated LiCl solution at 50 °C for one week. Elemental analysis confirmed that the chemical compositions of the cubic and tetragonal phases were $Li_6La_3Zr_2O_{11.5}$ and $Li_7La_3Zr_2O_{12}$, respectively.

1. Introduction

High lithium ion conducting solid electrolytes are considered to be the best candidate for the electrolyte of a large size rechargeable high energy density battery with regard to safety. Sold lithium ion conductors have been reported for a wide range of metal oxides and metal halides with different types of crystal [1] and amorphous structures [2]. Recently, Thokchom et al. reported that a lithium aluminum germanium phosphate glass-ceramic, $Li_{1.5}Al_{0.5}Ge_{1.5}(PO_4)_3$, exhibited lithium ion conductivity as high as 5×10^{-3} S cm^{-1} at room temperature [3]. However, this compound was unstable in direct contact with lithium metal and the interface resistance drastically increased just after contact of the electrolyte with Li metal [4]. On the other hand, lithium phosphorous oxynitride, $Li_3(P,N)O_4$, is stable in contact with Li metal and the stability window is as high as from 0 to 5 V vs. Li/Li$^+$; however, the electrical conductivity is as low as 10^{-6} S cm^{-1} at 25 °C [5]. Kanno and Murayama reported high lithium ion conduction for the $Li_{4-x}Ge_{1-x}P_xS_4$ solid with the thio-LISICON structure at 2.2×10^{-3} S cm^{-1} at room temperature [6], and Mizuno et al. found that Li_2S-P_2S_5 glass ceramics exhibit high conductivity of 3.2×10^{-3} S cm^{-1} at room temperature [7]. These sulfides are stable in contact with Li metal, but are extremely hydroscopic and produce H_2S as the reaction product with water.

Weppner and coworkers reported the garnet-type solid electrolyte of $Li_5La_3M_2O_{12}$ (M = Nb, Ta) exhibits high lithium ion conductivity and good stability in contact with Li metal [8,9]. The highest lithium ion conductivity reported among investigated systems with the garnet-related structure was 4×10^{-5} S cm^{-1} at 22 °C for $La_6BaLa_2Ta_2O_{12}$. This compound was stable against reaction with Li metal, moisture, and air. However, the conductivity of this compound is not sufficiently high to develop a high power density solid state battery. Recently, Murugan et al. [10] reported a new garnet-type lithium ion conducting solid electrolyte of $Li_7La_3Zr_2O_{12}$ (LLZ). The measured powder XRD patterns of this compound matched well with the standard pattern of the garnet-type cubic phase $Li_5La_3Nb_2O_{12}$, although the chemical formula of the cubic phase was not determined. The ionic conductivity of a sintered pellet (92% theoretical density) was reported to be 2.44×10^{-4} S cm^{-1} at 25 °C, which is quite attractive for a lithium battery electrolyte. This new garnet-type lithium conductor was found to be stable against molten lithium. However, the Li/LLZ/Li cell showed a high polarization potential at higher current drain [11]. The high polarization potential may be due to high interfacial resistance between Li metal and LLZ. More recently, Awaka et al. reported a $Li_7La_2Zr_2O_{12}$ garnet-related lithium ion conductor with tetragonal symmetry, which was synthesized at 980 °C [12]. The bulk and grain boundary electrical conductivities of the tetragonal phase were as low as 1.63×10^{-6} and 5.59×10^{-7} S cm^{-1} at 27 °C, respectively.

We have previously reported [13,14] a water stable lithium metal anode, which consisted of lithium metal, a polyethylene oxide based polymer electrolyte, and a water–stable lithium conducting solid electrolyte, $Li_{1.55}Ti_{1.75}Al_{0.25}Si_{0.3}P_{2.7}O_{12}$ (LTAP). The polymer electrolyte was used as an interface layer to prevent the reaction of lithium metal with the solid electrolyte, because the solid electrolyte is unstable in direct contact with lithium metal. If LLZ is stable in an aqueous electrolyte, then a water stable lithium electrode could be produced using LLZ without the polymer electrolyte interface, because LLZ is stable with lithium metal. A water stable lithium metal electrode could be widely used as the lithium electrode in a

* Corresponding author. Tel.:+ 81 59 231 9419; fax: +81 59 231 9478.
E-mail address: takeda@chem.mie-u.ac.jp (Y. Takeda).

0167-2738/$ – see front matter © 2010 Elsevier B.V. All rights reserved.
doi:10.1016/j.ssi.2010.12.010

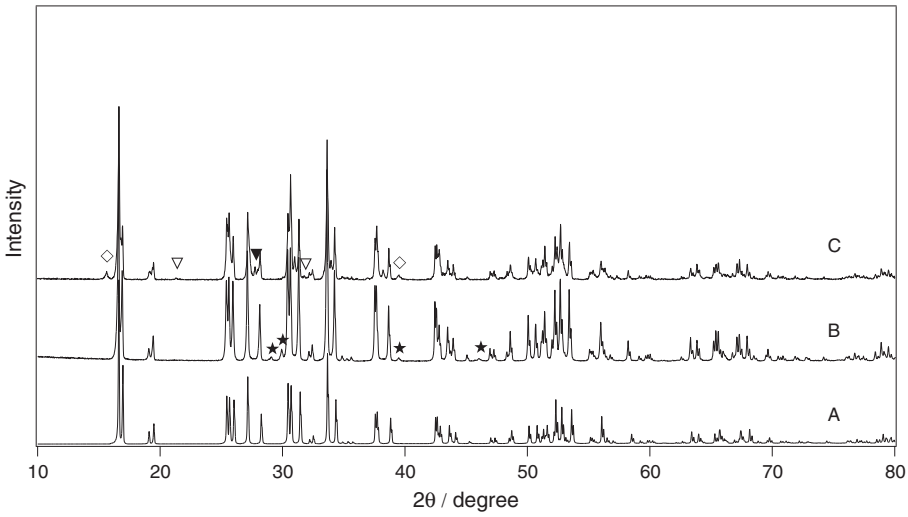

Fig. 1. XRD patterns of samples heated at 800 °C for 20 h. A: Simulated XRD pattern of the garnet-type tetragonal phase with a = 1.3134 and c = 1.2663 nm. B: Precursor composition of $Li_7La_3Zr_2O_{12}$ (t-LLZ-7). C: Precursor composition of $Li_{7.7}La_3Zr_2O_{12.35}$ (t-LLZ-8). ★: La_2O_3, ▼: $La_2O_2CO_3$, ▽: Li_2CO_3, : $La(OH)_3$.

high energy density lithium-air secondary battery [15–17]. In this study, we have prepared LLZ from a precursor obtained by the sol–gel method, and the atomic ratio of the garnet-type cubic and tetragonal phases were examined, in addition to the stability of LLZ in aqueous solutions.

2. Experimental

Precursors for the nominal chemical formula $Li_7La_3Zr_2O_{12}$ and for an approximately 10% excess lithium content ($Li_{8.05}La_3Zr_2O_{12.525}$ and $Li_{7.7}La_3Zr_2O_{12.35}$) in the starting materials were prepared by a conventional sol–gel method using citric acid. The corresponding quantities of chemical grade $LiNO_3$, $La(NO_3)_36H_2O$, and $ZrO(NO_3)H_2O$ were dissolved in water and then citric acid and ethylene glycol (1:1 mole ratio) were added into the solution. Water was added to completely dissolve the starting materials. The amounts of citric acid and ethylene glycol used were twice the total moles of cations in the precursor solution. The solution was stirred for several hours on a hot plate to produce a black solid. The obtained solid was heated again at 350 °C for 5 h in open air and then ground to fine powder. The powder was isostatically pressed into pellets prior to heating at 800 °C for 20 h. The obtained pellets were reground and again isostatically pressed to a pellet of 1.0 cm in diameter at 150 MPa. The pelletized samples were annealed at various temperatures in air. The pellets were covered with the mother powder for high temperature annealing.

X-ray diffraction (XRD) data were obtained using a Rigaku RINT 2500 with a rotating copper cathode. Elemental analysis of Li, La, Zr and Al in the samples obtained by various annealing conditions was carried out using inductively coupled plasma spectroscopy (ICP; Shimadzu ICPS 1000). The samples were completely resolved into a mixed solution of hydrochloric acid and nitric acid (3:1 volume ratio) before ICP analysis. The electrical conductivity of the sintered samples ca. 0.7 cm and 0.1 cm thick) with sputtered gold electrodes was measured using a Solartron 1260 frequency response analyzer in the frequency range of 0.1 Hz to 1 MHz and in the temperature range of 25 to 80 °C. Z-plot software was employed for data analysis.

Stability tests in aqueous solutions were conducted using sintered pellet samples. The pellets were immersed in aqueous solutions with saturated LiCl, 1 M LiOH and 0.1 M HCl at 50 °C for one week. The

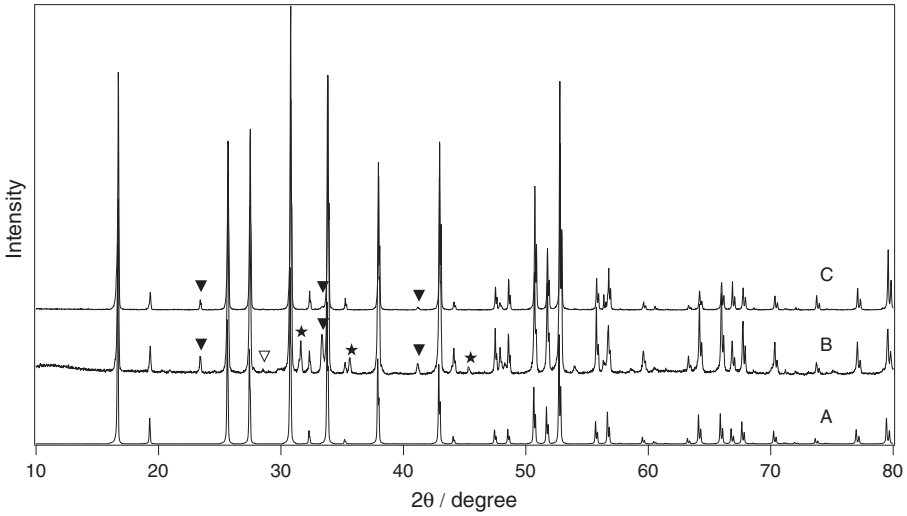

Fig. 2. XRD patterns of samples annealed at 1180 °C for 36 h. A: Simulated XRD pattern of the garnet-type cubic phase with a = 1.29682 nm. B: Precursor composition of $Li_7La_3Zr_2O_{12}$ (c-LLZ-7). C: Precursor composition of $Li_{8.05}La_3Zr_2O_{12.525}$ (c-LLZ-8). ▼: $LaAlO_3$ ▽: $La_2Zr_2O_7$ ★: unknown.

pellets immersed in these solutions were then dried under vacuum at 220 °C for several hours, and the changes in electrical conductivity, structure, and morphology after immersion were examined.

3. Results and discussion

Precursors with starting compositions of $Li_7La_3Zr_2O_{12}$, $Li_{7.7}La_3Zr_2O_{12.35}$, and $Li_{8.05}La_3Zr_2O_{12.525}$ were heated at 800 °C for 20 h in air. In some cases, the obtained samples were reground, repressed and heated again at 800 °C for 20 h. Fig. 1 shows XRD patterns of the heated products from precursor compositions of $Li_7La_3Zr_2O_{12}$ (t-LLZ-7) and $Li_{7.7}La_3Zr_2O_{12.35}$ (t-LLZ-8) along with that simulated based on the single crystal data for tetragonal $Li_7La_3Zr_2O_{12}$ with a = 1.3134 nm and c = 1.2663 nm from ref. [12]. The main diffraction lines correspond to the lines of the simulated pattern. In both product patterns, small amounts of extra peaks corresponding to unreacted precursors were observed. The observed lattice parameters for t-LLZ-7 were a = 1.3097 nm and c = 1.2660 nm, and those for t-LLZ-8 were a = 1.313 nm and c = 1.2677 nm. These values are almost the same as those for the single crystal. There was no significant difference observed in the XRD patterns of both t-LLZ-7 and t-LLZ-8. Even when prepared under lithium rich conditions, the obtained tetragonal phase had the same composition of t-LLZ-7. There was no significant lithium loss by heating at 800 °C as evidenced from thermogravimetric measurements.

The samples heated at 800 °C were ground again and the obtained powders were pressed into pellets under an isostatic pressure of 150 MPa and annealed at 1180 °C for 35 h under open air. Fig. 2 shows XRD patterns of the annealed samples with precursor compositions of $Li_7La_3Zr_2O_{12}$ (c-LLZ-7) and $Li_{8.05}La_2Zr_2O_{12.525}$ (c-LLZ-8) along with the simulated pattern. The XRD pattern of a simple garnet-type structure with a space group of Ia3d was simulated using structural parameters of La = 24c, Zr = 16c, O = 96c, and Li = 24d and 48d, where the lattice parameter of a = 1.29682 nm reported by Murugan et al. [10] was used. The observed XRD pattern of c-LLZ-8 is consistent with the simulated garnet-type structure, except for a trace impurity phase of $LaAlO_3$. The annealed low lithium content precursor, c-LLZ-7, has extra unknown diffraction peaks. The unknown phase may be produced by the lithium loss during the high temperature annealing. The lattice parameter of 1.2965 nm calculated for c-LLZ-8 is comparable with that reported previously [10].

The elemental contents of LLZ were analyzed using ICP and the results are summarized in Table 1. The ratio of Li/La/Zr in the low temperature tetragonal phase, t-LLZ, is 7/3.1/2. The content of La is slightly higher than that of the precursors and this may be due to experimental error. Awaka et al. measured the Li/La/Zr ratio in the $Li_7La_3Zr_2O_{12}$ tetragonal phase to be 7.36/3.16/2.0 using ICP [12]. Our result for the tetragonal phase is more close to the stoichiometric content. In the $Li_7La_3Zr_2O_{12}$ tetragonal phase, the samples prepared from the high lithium content precursor of $Li_{7.7}La_3Zr_2O_{12}$ showed the high content of Li: Li/La/Zr = 7.5/3.1/2.0. The high Li content may be due to impurity phases, such as Li_2O. The samples reported by Awaka et al. were prepared using starting materials with an approximately 10 wt.% excess of Li. On the other hand, the element ratio in the cubic phase is far from that in the precursor and Al is observed. The Al may come from the alumina vessel used for annealing at high temperatures. The mother powder covering the c-LLZ-8 pellets may react with the alumina vessel and the aluminum compound (finally as $LaAlO_3$) could then diffuse into the LLZ pellets. The content of La in c-LLZ-8 was modified by estimating the content of $LaAlO_3$ from XRD patterns and reducing the content of La in $LaAlO_3$. The modified Li/La/Zr ratio in c-LLZ-8 is 5.96/2.96/2.0. The lithium content of the cubic phase is lower compared to that of the tetragonal phase. The lithium content in the cubic phase was not dependent on the precursor composition. The sample with a precursor composition of $Li_7La_3Zr_2O_{12}$ annealed at 1180 °C has an element ratio of Li/La/Zr = 6.0/3.1/2.0, which was not modified by the Al content. The high temperature cubic phase showed no reversible phase transition to the tetragonal phase by annealing at 800 °C for a long period. These results suggest that c-LLZ and t-LLZ have different compositions of $Li_6La_3Zr_2O_{11.5}$ and $Li_7La_3Zr_4O_{12}$, respectively. The composition of the cubic phase was not reported in the previous studies [10,11]. Crystal structure analysis of cubic $Li_5La_3Ta_2O_{12}$ by neutron diffraction revealed that the occupancy of the lithium sites were 23.8% and octahedrally coordinated lithium was mainly disordered [18]. This structure could contain more lithium ions. Awaka et al. reported that $Li_6MLa_2O_{12}$ (M = Ca, Ba) had the same disordered lithium structure as cubic $Li_5La_3Ta_2O_{12}$ [19]. However, $Li_6La_3Zr_2O_{11.5}$ should have oxygen deficient sites in the structure.

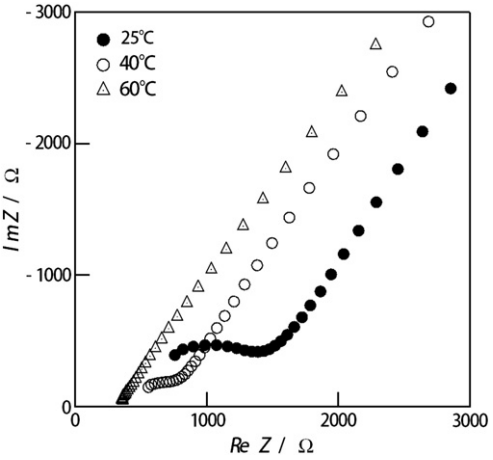

Fig. 3. Impedance spectra of c-LLZ-8 at 25, 40, and 60 °C.

Table 1
Elemental analysis of LLZ.

Precursor composition	$Li_{8.05}La_3Zr_2O_{12.525}$	$Li_7La_3Zr_2O_{12}$	$Li_{7.7}La_3Zr_2O_{12.35}$	$Li_7La_3Zr_2O_{12}$
Annealing temperature (°C)	1180	1180	800	800
Crystal symmetry	Cubic	Cubic	Tetragonal	Tetragonal
Li atom ratio	5.96 (5.96[a])	6.0	7.5	7.0
La atom ratio	3.23 (2.96[a])	3.1	3.1	3.1
Zr atom ratio	2.00 (2.00[a])	2.0	2.0	2.0
Al atom ratio	0.23	–	–	–

[a] Modified atom ratio — not measured.

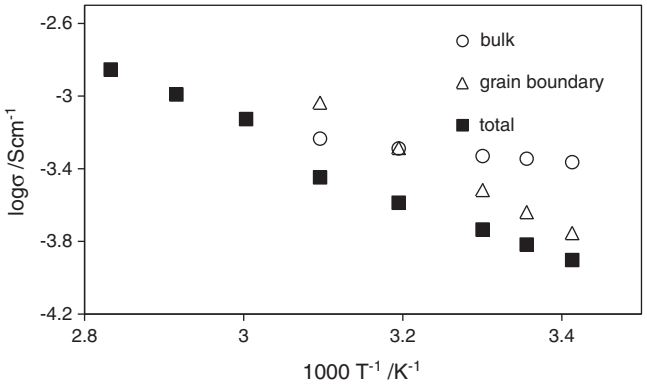

Fig. 4. Temperature dependence of the total, bulk and grain boundary conductivity of c-LLZ-8.

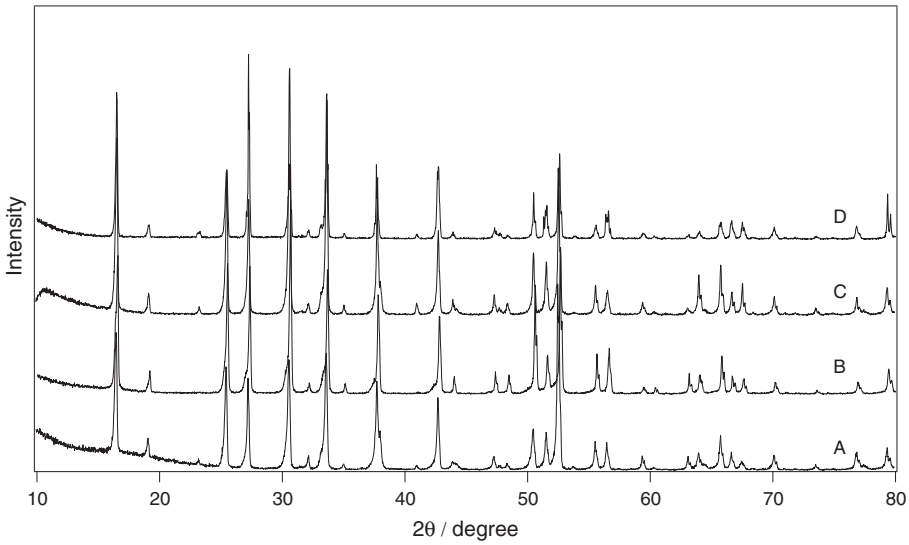

Fig. 5. XRD patterns of c-LLZ-8 after immersion in various aqueous solutions at 50 °C for one week. A: LiCl saturated aqueous solution. B: H_2O. C:1 M LiOH aqueous solution. D: 0.1 M HCl aqueous solution.

More precise study of the composition and the cubic phase crystal structure is required.

The electrical conductivity of the garnet-related cubic $Li_7La_3Zr_2O_{12}$ phase was reported to be around 2×10^{-4} S cm^{-1} at room temperature [10,11]. The impedance plot by Murugan et al. [10] showed two clear semicircles in the frequency range of 5 Hz to 13 MHz. The high frequency and low frequency semicircles were attributed to the contribution of bulk resistance and grain boundary resistance, respectively. The bulk conductivity of the cubic $Li_7La_3Zr_2O_{12}$ phase was estimated to be 3.97×10^{-4} S cm^{-1} at 18 °C from the impedance plots. The impedance profile of $Li_7La_3Zr_2O_{12}$ by Kaeriyama et al. [11] showed only one semicircle in the frequency range of 0.1 Hz to 13 MHz. The grain boundary resistance of a sintered sample is dependent on the preparation method. Fig. 3 shows typical impedance profiles at various temperatures in the frequency range of 0.1 Hz to 1 MHz for c-LLZ-8 annealed at 1180 °C for 36 h under air, where the precursor composition was $Li_{8.05}La_3Zr_2O_{12.525}$. The impedance profile shows a semicircle, which is attributed to the grain boundary resistance of the

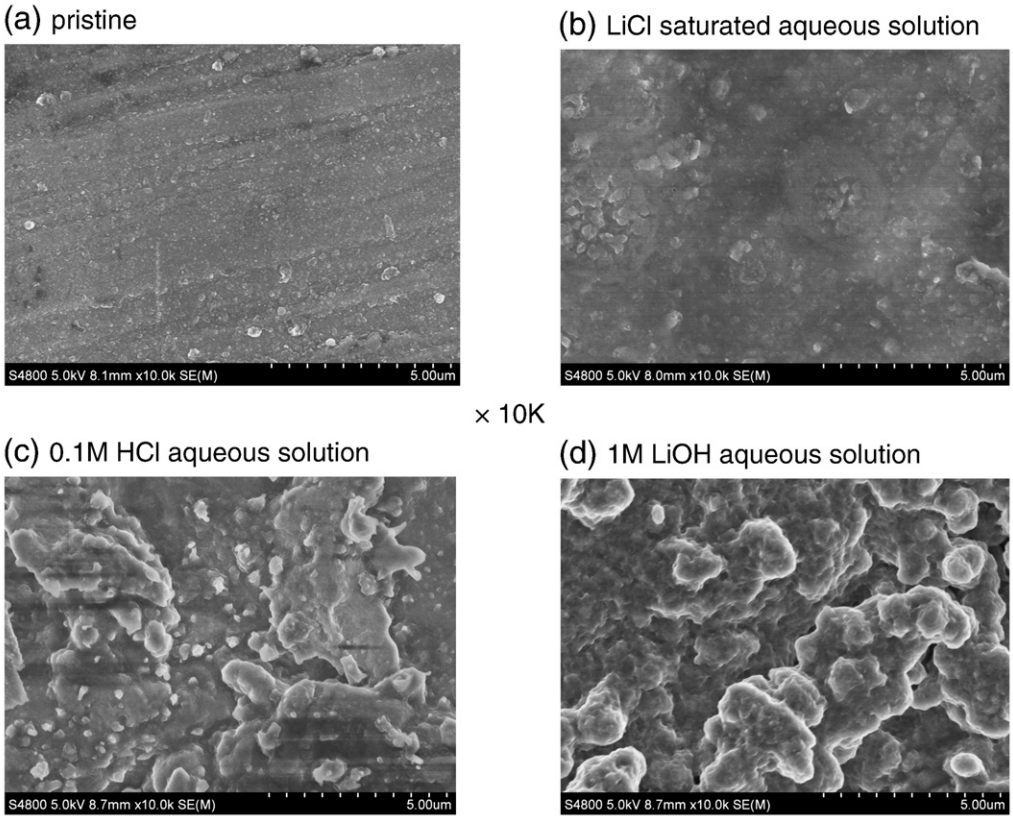

Fig. 6. SEM images of c-LLZ-8 surfaces after immersion in aqueous solutions at 50 °C for one week. (a) Pristine, (b) saturated LiCl, (c) 0.1 M HCl, and (d) 1 M LiOH aqueous solutions.

sample. The intercept of the semicircle on the real axis at high frequency represents the bulk resistance [20]. The bulk resistance and the grain boundary resistance at 25 °C were estimated to be 95 Ω cm^2 and 394 Ω cm^2, or 5.69×10^{-4} S cm^{-1} and 1.39×10^{-4} S cm^{-1}, respectively. The bulk conductivity is comparable and the grain boundary conductivity is lower than those reported previously by Murugan et al. [10]. The low conductivity (high resistance) of the grain boundary may be due to the segregation of high resistance impurity phases, such as $LaAlO_3$, at the grain boundary. The temperature dependence of the grain boundary conductivity and the bulk conductivity of c-LLZ-8 are shown in Fig. 4. The temperature dependence looks like to be divided two parts of a low temperature and a high temperature regions, but it may be due to the uncertain of the estimation of the resistance from the impedance profile at low temperature. The activation energies for conduction are 7.7 kJ mol^{-1} for the bulk conductivity and 35.6 kJ mol^{-1} for the total conductivity. The activation energy for the total conductivity is comparable, and that for the bulk conductivity is lower than those reported previously [10]. The low activation energy for the bulk conductivity could be explained by more available sites for lithium ion diffusion [18]. The electrical conductivity of the tetragonal t-LLZ phase was measured to be 4.4×10^{-7} S cm^{-1} for the bulk and 2.8×10^{-7} S cm^{-1} for the grain boundary at 25 °C. The activation energy for bulk conduction in t-ZZL was estimated to be 52.3 kJ mol^{-1}. The low conductivity and high activation energy for conduction in the tetragonal garnet-type structure could be explained by the ordered structure [21].

Murugan et al. reported that garnet-related $Li_7La_3Zr_2O_{12}$ was stable against molten lithium and also chemically stable when exposed to moisture and air for several weeks [10]. The stability of $Li_7La_3Zr_2O_{12}$ in aqueous solutions has not been examined yet. The stability of lithium conducting solid electrolytes in aqueous solutions is necessary for application as a protective layer for a water stable lithium electrode [14]. In this study, the stability of c-LLZ-8 with high electrical conductivity was examined in various aqueous solutions.

Fig. 5 shows XRD patterns of c-LLZ-8 after immersion in aqueous solutions of saturated LiCl, H_2O, 1 M LiOH, and 0.1 M HCl at 50 °C for one week. No significant change in the XRD patterns was observed for all samples immersed in these aqueous solutions. Therefore, high conductivity c-LLZ is stable in acidic and alkaline aqueous solutions, with respect to the structural information from XRD patterns. Fig. 6 shows SEM images of c-LLZ-8 after immersion in these aqueous solutions at 50 °C for one week. No significant change in the surface morphology was observed for the samples immersed in saturated LiCl aqueous solution. However, those immersed in 0.1 M HCl and 1 M LiOH aqueous solutions showed a significant change in surface morphology due to reaction with the solution. Therefore, c-LLZ-8 may be unstable in these solutions and react, but the reaction product was not observed by XRD. These results are comparable to those for the water stable LTAP electrolyte. A trace amount of decomposition product of Li_3PO_4 and significant surface morphology change was observed for LTAP immersed in a 1 M LiOH aqueous

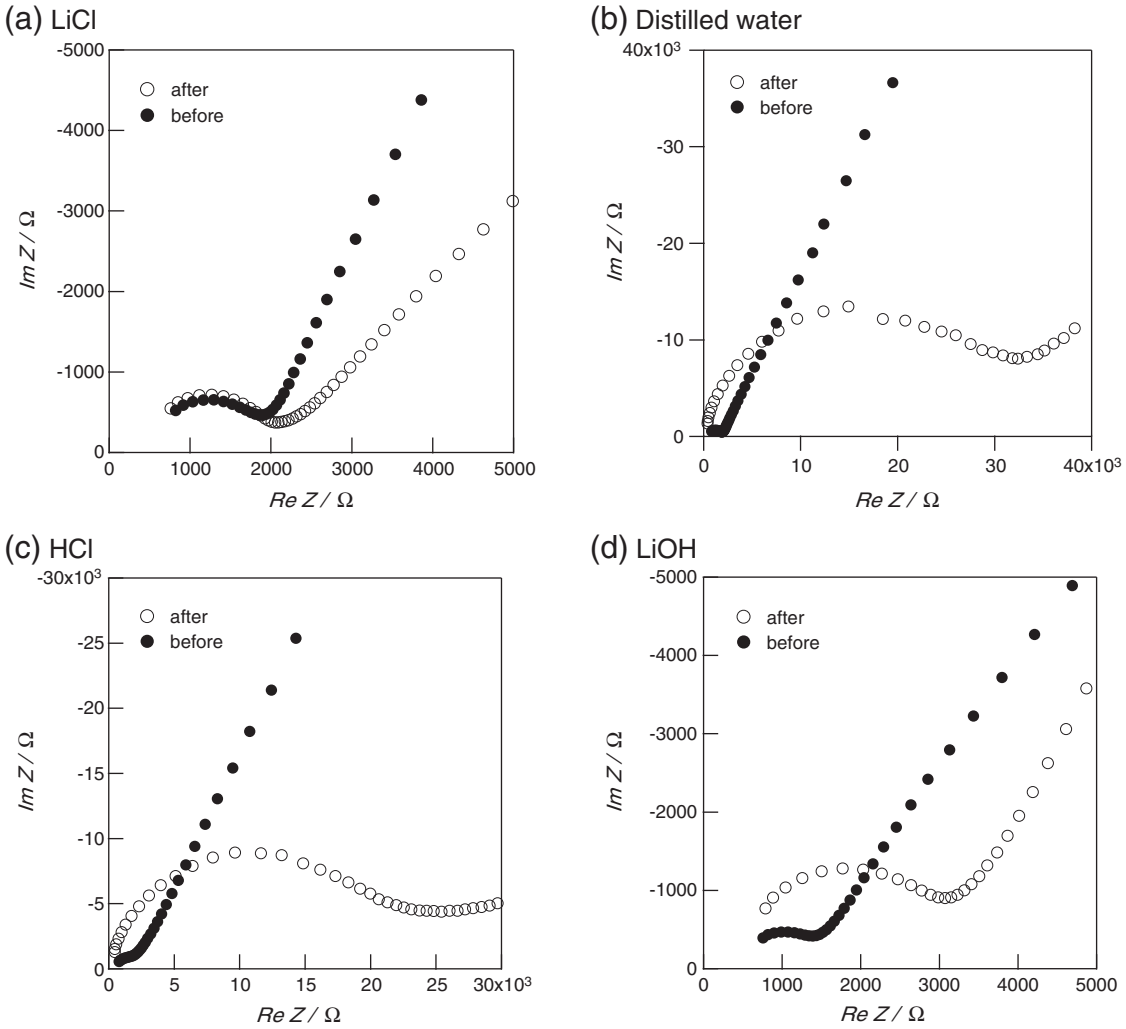

Fig. 7. Impedance spectra of c-LLZ-8 measured at 25 °C after immersion in (a) saturated LiCl aqueous solution, (b) H_2O, (c) 1 M LiOH, and (d) 0.1 M HCl aqueous solutions at 50 °C for one week.

solution at 50 °C for one week. However, no reaction product was observed after immersion of LTAP in 0.1 M HCl aqueous solution at 50 °C for one week, although the smooth surface of the pristine LTAP was etched in 0.1 M HCl solution [22]. These results suggest that the cubic garnet-related $Li_6La_3Zr_2O_{11.5}$ is more stable in acid and basic aqueous solutions than LTAP.

Electrical conductivity changes due to immersion of c-LLZ-8 in various aqueous solutions at 50 °C for one week were examined. Fig. 7(a) shows a typical impedance plot measured at 25 °C for c-LLZ-8 after immersion in saturated LiCl aqueous solution at 50 °C for one week. No significant change in the impedance profile was observed when compared with that of the pristine c-LLZ-8, as shown in the figure. The grain and grain boundary conductivity were almost the same before and after immersion in saturated LiCl aqueous solution. Typical impedance profiles of c-LLZ-8 after immersion in H_2O, 1 M LiOH, and 0.1 M HCl aqueous solutions at 50 °C for one week are shown in Fig. 7-(b), (c) and (d), respectively. The bulk conductivity of c-LLZ-8 after immersion in 1 M LiOH aqueous solution was estimated to be 5.8×10^{-4}S cm^{-1} at 25 °C, which is comparable to that of the pristine c-LLZ. However, the grain boundary conductivity decreased to 7.9×10^{-5} Scm^{-1}. c-LLZ-8 immersed in 1 M HCl aqueous solution and in H_2O also showed no change in the bulk conductivity, but a significant decrease in the grain boundary conductivity was evident. The increase in the grain boundary resistance could be explained by the segregation of high resistance decomposition products, which could not be clearly detected by XRD. We could conclude that c-LLZ-8 is stable in saturated LiCl aqueous solution with respect to the structure and electrical conductivity, and is unstable in water, acid and alkaline solutions. The stability of LLZ in saturated LiCl aqueous solution is quite attractive for the protect layer of lithium metal, because the saturated LiCl aqueous solution is acceptable for the electrolyte in lithium-air secondary batteries[22]. The stability of LLZ in aqueous solutions is similar to that of the NASICON-type lithium conducting solid, LTAP, which is unstable in acid and alkaline solutions and stable in the saturated LiCl aqueous solution. However, LTAP is more stable in water [23].

4. Conclusion

A high lithium ion conducting solid electrolyte, $Li_6La_3Zr_2O_{11.5}$, with the garnet-related structure was prepared from precursors obtained by a sol–gel method.

XRD patterns of samples annealed at 800 °C for 20 h indicated tetragonal symmetry and those annealed at 1180 °C for 32 h had cubic symmetry. Elemental analysis suggested that the chemical formulae of the cubic and tetragonal phases were $Li_6La_3Zr_2O_{11.5}$ and $Li_7La_3Zr_2O_{12}$, respectively. The cubic phase exhibited a high bulk conductivity of 6.5×10^{-4} S cm^{-1} at 25 °C and showed no conductivity change after immersion in saturated LiCl aqueous solution at 50 °C for one week. The excellent stability in aqueous solution with LiCl suggests that $Li_6La_3Zr_2O_{11.5}$ would be a good candidate for the protective layer of a water stable lithium metal electrode for lithium-air batteries as proposed [14]. $Li_6La_3Zr_2O_{11.5}$ is more acceptable than LTAP, which was used previously as a water stable solid lithium ion conductor in a water stable lithium metal electrode, due to the stability of $Li_6La_3Zr_2O_{11.5}$ in contact with metallic lithium compared with the instability of LTAP.

Acknowledgments

This research was sponsored by a Grant-in-Aid for Scientific Research (B 22350091) from the Ministry of Education, Culture, Sports, Science and Technology of Japan, and the New Energy and Industrial Technology Development Organization (NEDO) of Japan under the project, Development of High Performance Battery System for Next-Generation Vehicles.

References

[1] A.R. West, in: P.G. Bruce (Ed.), Solid State Electrochemistry, Cambridge University Press, Cambridge, 1995, p. 7.
[2] J.L. Souquet, in: P.G. Bruce (Ed.), Solid State Electrochemistry, Cambridge University Press, Cambridge, 1995, p. 74.
[3] J.S. Thokchom, N. Gupta, K. Kumar, J. Electrochem. Soc. 155 (2008) A915.
[4] X. Xu, Z. Wen, X. Wu, X. Yang, Z. Gu, J. Am. Ceram. Soc. 90 (2007) 2802.
[5] J.B. Bates, N.J. Dudney, G.R. Gruzalski, R.A. Zuhr, A. Choudhury, C.F. Luck, Solid State Ionics 53–56 (1992) 647.
[6] R. Kanno, M. Murayama, J. Electrochem. Soc. 148 (2001) A742.
[7] F. Mizuno, A. Hayashi, K. Tadanaga, M. Tatsumisako, Adv. Mater. 17 (2005) 918.
[8] W. Thangadurai, H. Kaack, W. Weppner, J. Am. Ceram. Soc. 86 (2003) 437.
[9] R. Murugan, V. Thangadurai, W. Weppner, J. Electrochem. Soc. 155 (2008) A90.
[10] R. Murugan, V. Thangadurai, W. Weppner, Angew. Chem. Int. Ed. 46 (2007) 7778.
[11] A. Kaeriyama, H. Munakata, K. Kajihara, K. Kanamura, Y. Sato, T. Yoshida, J. Electrochem. Soc. 157 (2010) A1078.
[12] J. Awaka, N. Kijima, H. Hayakawa, J. Akimoto, J. Solid State Chem. 182 (2009) 2046.
[13] N. Imanishi, S. Hasegawa, T. Zhang, A. Hirano, Y. Takeda, O. Yamamoto, J. Power Sources 189 (2008) 371.
[14] T. Zhang, N. Imanishi, S. Hasegawa, A. Hirano, J. Xie, Y. Takeda, O. Yamamoto, J. Electrochem. Soc. 155 (2008) A965.
[15] A. Krsytsberg, Y. Ein-Eli, J. Power Sources 196 (2011) 886.
[16] K.M. Abraham, Z. Jiang, J. Electrochem. Soc. 143 (1996) 1.
[17] A. Debart, A.J. Paterson, J. Bao, P.G. Bruce, Angew. Chem. Int. Ed. 47 (2008).
[18] E.J. Cussen, Chem. Commun. (2006) 412.
[19] J. Awaka, N. Kijima, Y. Takahashi, H. Hayakawa, J. Akimoto, Solid State Ionics 180 (2009) 602.
[20] P.C. Bruce, A.R. West, J. Electrochem. Soc. 130 (1983) 652.
[21] V. Thangadura, S. Adams, W. Weppner, Chem. Mater. 16 (2004) 2998.
[22] S. Hasegawa, N. Imanishi, T. Zhang, J. Xie, A. Hirano, Y. Takeda, O. Yamamoto, J. Power Sources 189 (2009) 371.
[23] Y. Shimonishi, T. Zhang, N. Imanishi, A. Hirano, Y. Takeda, O. Yamamoto, The 51th Battery Symposium in Japan, Nagoya, Japan, Abst. # 3B24, 2010.